HHS Public Access

Author manuscript

Sci Signal. Author manuscript; available in PMC 2019 April 05.

Published in final edited form as:

Sci Signal. ; 7(325): ra45. doi:10.1126/scisignal.2004882.

* T Cell Receptor Signals to NF-κB Are Transmitted by a Cytosolic p62-Bcl10-Malt1-IKK Signalosome

Suman Paul[1,*], **Maria K. Traver**[1], **Anuj K. Kashyap**[1,†], **Michael A. Washington**[1,‡], **Joseph R. Latoche**[1,§], and **Brian C. Schaefer**[1,2,‖]

[1]Department of Microbiology and Immunology, Uniformed Services University, Bethesda, MD 20814, USA.

[2]Center for Neuroscience and Regenerative Medicine, Uniformed Services University, Bethesda, MD 20814, USA.

Abstract

Antigen-mediated stimulation of the T cell receptor (TCR) triggers activation of nuclear factor κB (NF-κB), a key transcriptional regulator of T cell proliferation and effector cell differentiation. TCR signaling to NF-κB requires both the Carma1-Bcl10-Malt1 (CBM) complex and the inhibitor of κB (IκB) kinase (IKK) complex; however, the molecular mechanisms connecting the CBM complex to activation of IKK are incompletely defined. Here, we found that the active IKK complex is a component of a TCR-dependent cytosolic Bcl10-Malt1 signalosome containing the adaptor protein p62, which forms in effector T cells. Phosphorylated IκBα and NF-κB were transiently recruited to this signalosome before NF-κB translocated to the nucleus. Inhibiting the activity of the kinases TAK1 or IKK blocked the phosphorylation of IKK, but not the formation of p62-Bcl10-Malt1 clusters, suggesting that activation of IKK occurs after signalosome assembly. Furthermore, analysis of T cells from p62-deficient mice demonstrated that the p62-dependent clustering of signaling components stimulated activation of NF-κB in effector T cells. Thus, TCR-stimulated activation of NF-κB requires the assembly of cytosolic p62-Bcl10-Malt1-IKK signalosomes, which may ensure highly regulated activation of NF-κB in response to TCR engagement.

‖Corresponding author. Brian.Schaefer@usuhs.edu.

*Current address: Department of Internal Medicine, University of Toledo Medical Center, 3000 Arlington Avenue, Toledo, OH 43614, USA.

†Current address: Howard Hughes Medical Institute (HHMI), Janelia Farm Research Campus, Molecular Biology Shared Resource, 19700 Helix Drive, Ashburn, VA 20147, USA.

‡Current address: Tripler Army Medical Center, Department of Clinical Investigation, 1 Jarrett White Road, Honolulu, HI 96818, USA.

§Current address: Windber Research Institute, Integrative Cardiac and Metabolic Health Program, 620 7th Street, Windber, PA 15963, USA.

Author contributions: S.P. and B.C.S. designed the experiments and wrote the manuscript; J.R.L. maintained and genotyped the mice; and S.P., M.K.T., A.K.K., and M.A.W. performed experiments and collected data. The views expressed are those of the authors and do not necessarily reflect those of the Uniformed Services University or the Department of Defense.

Competing interests: The authors declare that they have no competing interests.

Introduction

Specific engagement of antigen-bound major histocompatibility complex (MHC) proteins on the surface of antigen-presenting cells (APCs) by the T cell receptor (TCR) initiates a signaling cascade that activates nuclear factor κB (NF-κB), a critical transcriptional regulator of T cell proliferation and differentiation programs (1). Early TCR-proximal signals lead to activation of protein kinase C θ (PKCθ), which phosphorylates the large adaptor protein Carma1 to stimulate its association with a pre-existing complex of the small adaptor Bcl10 and the protease Malt1 to form the "CBM" complex. Assembly of the CBM complex is followed by activation of the inhibitor of κB (IκB) kinase (IKK), which is composed of the serine and threonine kinases IKKα and IKKβ and a non-catalytic regulatory subunit (IKKγ). Activated IKK phosphorylates the NF-κB inhibitor, IκBα, leading to the polyubiquitination and degradation of IκBα, thereby freeing NF-κB to translocate to the nucleus to activate target genes. Whereas it is known that the constituents of the CBM complex are required for the activation of IKK, the molecular mechanism by which CBM proteins interact with IKK remains incompletely understood (2).

Accumulating data from our group and others suggests that signaling from the CBM complex to IKK involves a progressive series of steps, which incorporate discrete membrane-proximal and cytosolic signaling platforms. Biochemical studies have shown that PKCθ and Carma1 are located on lipid rafts in activated T cells (3), together with a fraction of Bcl10, Malt1, and IKK (4, 5). However, the IκBα–NF-κB complex is present only in the cytosol. Thus, current data do not explain how membrane-associated upstream signal transducers transmit activating signals to the cytosolic IκBα-NF-κB complex (5). A study suggests that the early CBM complex matures to form the Bcl10-Malt1 complex, and that this latter complex inducibly interacts with IκBα (6). Additionally, imaging studies from our group identified TCR-induced cytosolic clusters of Bcl10 and Malt1, called POLKADOTS (7-9), which are sites of enriched interactions between Bcl10 and the E3 ubiquitin ligase TRAF6 (tumor necrosis factor receptor-associated factor 6) (8). The presence of these signaling clusters is highly correlated with the extent of nuclear translocation of NF-κB (10), suggesting a role for POLKADOTS in activating NF-κB.

POLKADOTS are de novo cytoplasmic aggregates that require TCR-dependent lysine-63 (K63)-mediated polyubiquitination of Bcl10. A structural study demonstrated that Bcl10 forms filamentous structures in the presence of the active form of Carma1, and that the ability to form filaments correlates with the ability to activate NF-κB (11). Our data suggest that K63-polyubiquitination of Bcl10 causes these filaments to cluster around pre-existing aggregates ("speckles") of the ubiquitin-binding adaptor protein, p62 (also known as SQSTM-1), to form the POLKADOTS structures. Knockdown of p62 blocks both the formation of POLKADOTS and the activation of NF-κB (7). These data are consistent with a study of $p62^{-/-}$ mice, which showed that p62 contributes to TCR-dependent IKK activation and T cell differentiation (12). Together, these biochemical, imaging, and genetic data are consistent with the hypothesis that p62, Bcl10, and Malt1 form a cytosolic complex (the POLKADOTS signalosome) that is responsible for transducing activating signals to IKK and NF-κB.

Here, we sought to provide direct evidence that TCR-induced cytosolic POLKADOTS clusters direct the activation of NF-κB. Our data demonstrate that after TCR stimulation, activated IKK localized to cytosolic POLKADOTS, and not to the membrane-associated CBM complex. Phosphorylated IκBα and NF-κB were also transiently present at the POLKADOTS structures, before the nuclear translocation of NF-κB occurred. Finally, genetic data demonstrated that cluster formation and NF-κB activation were highly dependent on p62 abundance. These data establish that TCR signaling drives the assembly of cytosolic p62-Bcl10-Malt1-IKK clusters or signalosomes that direct the activation of NF-κB.

Results

Cytosolic Bcl10-p62 clusters colocalize with phosphorylated IKK and TRAF6 in response to TCR stimulation

In experiments with primary effector T cells and the murine T helper 2 (T_H2) clone, D10, we previously demonstrated that stimulation with cognate antigen or anti-CD3 antibody stimulates the formation of cytosolic aggregates containing Bcl10 and Malt1. These structures, which we have named POLKADOTS, coalesce around pre-existing “speckles” of the adaptor protein p62 in a manner dependent on the TCR-dependent, K63-linked polyubiquitination of Bcl10 (7, 8). To ascertain the subcellular location of key mediators in the TCR–NF-κB pathway with respect to the cytosolic Bcl10 clusters, we stimulated D10 cells with antigen-loaded CH12 cells, which are an I-A^k-expressing murine B cell line. We then used confocal microscopy to image cyan fluorescent protein (CFP)-tagged PKCθ (PKCθ-CFP), yellow fluorescent protein (YFP)-tagged Bcl10 (Bcl10-YFP), and endogenous Carma1 and p62. At 10 and 20 min after stimulation of the D10 cells, PKCθ and Carma1 translocated to the immunological synapse (Fig. 1A), consistent with previous findings (3). Whereas some conjugates exhibited prominent colocalization between Bcl10 and PKCθ in D10 cells at the immunological synapse, as we previously reported (13), all conjugates (defined as D10-CH12 couples with PKCθ translocation at the immunological synapse) exhibited localization of Bcl10 within cytosolic aggregates that colocalized with p62 (7) in the antigen-activated cells (Fig. 1, A and B).

Our previous fluorescence resonance energy transfer (FRET) analyses demonstrated that Bcl10 is closely associated with TRAF6 in the POLKADOTS structures (8). Because TRAF6 is involved in recruiting and ubiquitinating IKK (1, 14), and because phosphorylated IKK (pIKK) is detected solely in the cytosol (5), we hypothesized that IKK is activated upon association with the cytosolic Bcl10-Malt1-p62–containing POLKADOTS structures. Staining with an antibody that specifically recognizes pIKKα/β (IKKα and IKKβ phosphorylated at residues Ser^{176} and Ser^{180}) revealed no apparent specific signal in unstimulated cells (Fig. 1C), although non-specific staining of the plasma membrane was observed in all cells. At 20 min and 2 hours after stimulation, we observed that pIKKα/β co-localized with the cytosolic Bcl10 clusters, but not with PKCθ at the immunological synapse (Fig. 1, C and D). Total IKKβ was present in cytosolic aggregates both before and after stimulation with antigen (Fig. 1D). Close inspection of the imaging data revealed that pIKKα/β staining was consistently adjacent to, but rarely overlapping with, total IKKβ

staining (Fig. 1D and fig. S1A), suggesting that the ρIKKα/β at POLKADOTS was distinct from the pool of IKKβ aggregates found in T cells before stimulation. The lack of overlap between pIKKα/β and total IKKβ staining was further confirmed by staining with a distinct IKKβ monoclonal antibody (fig. S1B). Staining with an anti-TRAF6 antibody also showed the TCR-induced redistribution of TRAF6 from a diffuse and primarily cytoplasmic localization in unstimulated cells to a punctate distribution that overlapped with Bcl10 and Malt1 in POLKADOTS 20 min after TCR stimulation with anti-CD3 antibody (Fig. 1E), with less prominent colocalization at the 2-hour time point (fig. S1C).

To confirm these data in primary T cells, we stimulated in vitro differentiated $CD4^+$ T_H2 effector cells with anti-CD3 and anti-CD28 antibodies (anti-CD3/28), followed by staining for endogenous Bcl10, p62, and pIKK proteins. At 20 min after stimulation, endogenous Bcl10 clusters were co-localized with p62 speckles, and pIKK was specifically localized to these p62-Bcl10 aggregates (Fig. 1F). Thus, the phenomenon of TCR-dependent colocalization of pIKK and cytosolic Bcl10 clusters was not only observed in D10 cells that over-expressed Bcl10 protein, but also occurred at clusters of endogenous Bcl10 in primary effector T cells. Together, these data suggest that IKK is recruited to and phosphorylated at the POLKADOTS structures shortly after TCR stimulation.

Activation of NF-κB occurs at the POLKADOTS signalosome

Once activated, the IKK holoenzyme phosphorylates IκBα, targeting IκBα for proteasomal degradation, thereby enabling the nuclear translocation of NF-κB. Because of the rapid kinetics of proteasomal degradation, ρIκBα is abundant only for a short period of time after TCR stimulation. Accordingly, at 10 min after stimulation of D10 cells with anti-CD3 antibody, we detected pIκBα that co-localized with Bcl10, Malt1, and pIKK (Fig. 2A). The pIκBα signal was undetectable by 20 min after stimulation, presumably because of its rapid proteasomal degradation, consistent with a previous report of IκBα degradation kinetics in D10 cells and primary T cells (7). These data suggest that IκBα is transiently recruited to the POLKADOTS structures, where it is phosphorylated by IKK, which stimulates its proteasomal degradation.

The NF-κB family consists of five proteins that exist as homo- or heterodimers (15), with RelA(p65)-p50 being the most common activating heterodimer. In unstimulated T cells, NF-κB resides in the cytosol, bound to IκBα. The degradation of IκBα unmasks a nuclear localization signal, which enables NF-κB to enter the nucleus, where it promotes the transcription of target genes. Because we detected pIκBα co-localized with Bcl10-Malt1 clusters, we hypothesized that RelA should be present contemporaneously. Imaging analysis revealed a homogenous cytosolic distribution of RelA before T cell stimulation (Fig. 2B). After 10 min of stimulation, either with antigen-loaded APCs or with anti-CD3 antibody, we observed that RelA co-localized with cytosolic Bcl10-Malt1 aggregates, but was not yet translocated to the nucleus (Fig. 2, B and C). By 20 min after stimulation, RelA was no longer colocalized with the POLKADOTS structures, but was enriched in the nucleus, consistent with our previous observations that IκBα degradation and NF-κB activation occur between 10 and 20 min after stimulation of the TCR on D10 cells (7, 10). Thus, RelA is transiently present at the POLKADOTS structures before it undergoes nuclear translocation.

The inhibition of either IKK or TAK1 blocks IKK phosphorylation at cytosolic Bcl10 signalosomes, causing reduced RelA activation

To further establish a mechanistic link between the IKK phosphorylation observed at the p62-Bcl10-Malt1 clusters (POLKADOTS) and the nuclear translocation of RelA, we treated D10 cells with BAY 11-7082 (BAY 11) or 5Z-7-oxozeaenol (5 oxo). BAY 11 is an inhibitor of IKK, which we used because a previous study suggests that trans-autophosphorylation of IKKβ participates in its activation (16). 5 oxo is a specific inhibitor of TAK1, a kinase identified as an essential activator of IKK phosphorylation in the TCR-NF-κB pathway (17). After stimulation with anti-CD3 antibodies, D10 cells treated with either BAY 11 or 5 oxo showed reduced phosphorylation of IKKα/β without having altered TCR-dependent phosphorylation of extracellular signal–regulated kinases 1 and 2 (ERK1/2) (Fig. 3A), consistent with a previous study (17).

Confocal microscopy analysis of antigen-stimulated D10 cells revealed that although inhibition of either IKK or TAK1 did not affect the translocation of PKCθ to the immunological synapse or the formation of Bcl10 clusters (Fig. 3B), BAY 11– and 5 oxo–treated D10 cells exhibited decreased pIKKα/β staining at Bcl10 clusters compared to those in vehicle-treated cells (Fig. 3B). These data also demonstrated that the observed anti-pIKK plasma membrane staining is non-specific, as it was not affected by BAY 11- or 5 oxo (Fig. 3B and fig. S2A). Additionally, both BAY 11 and 5 oxo blocked the nuclear translocation of RelA in D10 cells stimulated with antigen-loaded APCs or anti-CD3 antibody (Fig. 3, C and D), without apparently altering the translocation of PKCθ to the immunological synapse (Fig. 3C) or the formation of Bcl10 clusters (Fig. 3, C and D). Unstimulated, 5 oxo–treated D10 cells exhibited no change in the distribution of PKCθ-CFP, Bcl10-YFP, or endogenous RelA as compared to cells treated with vehicle (DMSO) alone (fig. S2, B and C). Quantification of microscopy data demonstrated a statistically significant reduction in the ratio of nuclear to cytosolic RelA in BAY 11– or 5 oxo–treated cells after stimulation with either antigen-loaded APCs or anti-CD3 antibody (Fig. 3E). Together, these observations suggest that inhibition of IKK or TAK1 activity prevents the efficient TCR-dependent phosphorylation of IKK. These data furthermore demonstrate that phosphorylation of IKK and activation of RelA are downstream of the translocation of PKCθ to the immunological synapse and the clustering of Bcl10 in POLKADOTS.

Loss of p62 blocks Bcl10 clustering, IKK phosphorylation, and RelA nuclear translocation in effector T cells

Studies suggest that p62 is required for the activation of NF-κB in differentiated effector T cells, but not in naïve T cells (12), which may reflect the fact that naïve cells have little or no p62 (18). Indeed, upon stimulation of wild-type primary $CD4^+$ T cells, we observed that p62 was low in abundance in primary $CD4^+$ T cells, and that there was a substantial increase in its abundance at 24 and 48 hours after stimulation with anti-CD3 and anti-CD28 antibodies (Fig. 4A), consistent with previous studies (12, 18). Moreover, we observed similar clustering of Bcl10 and ρIKKα/β beneath the capped TCR of naïve wild-type and $p62^{-/-}$ T cells, further suggesting that p62 does not play an essential role in the TCR-dependent activation of NF-κB in naïve T cells (Fig. 4B).

Two observations suggest that the TCR-dependent activation of NF-κB changes from being p62-independent in naïve T cells to being p62-dependent in effector T cells (2). First, whereas naïve $p62^{-/-}$ $CD4^+$ T cells exhibit normal IKK phosphorylation in response to anti-CD3/28 antibodies, by 24 hours after stimulation (by which time naïve $CD4^+$ T cells have differentiated into IL-2-producing effector T cells), $p62^{-/-}$ $CD4^+$ T cells fail to activate IKK (12). Second, the nuclear translocation of RelA in response to stimulation with anti-CD3 antibody is blocked in D10 cells in which p62 is knocked down (7). The implication of these observations is that differentiated T cells require one or more functions of p62 for the activation of IKK and NF-κB.

To establish a mechanistic relationship between p62 abundance and the activation of NF-κB in effector T cells, we assessed the extent of IKK activation in the presence and absence of p62. Western blotting analysis demonstrated minimal IKK phosphorylation in $p62^{-/-}$ T_H2 cells compared to that in wild-type T_H2 cells in response to anti-CD3/CD28 antibodies (Fig. 4C). In addition, the stimulation of wild-type or $p62^{-/-}$ T_H2 cells with APCs loaded with SEB (*Staphylococcus* enterotoxin B) resulted in no difference in the translocation of PKCθ to the plasma membrane (Fig. 4, D and E), indicating that membrane-proximal TCR–NF-κB signaling events were not affected by the loss of p62. However, cytosolic Bcl10 clustering was substantially impaired in $p62^{-/-}$ T cells compared to that in wild-type T cells in response to stimulation with antigen-loaded APCs or anti-CD3/28 antibodies (Fig. 4, E to G), consistent with our previous observations of reduced formation of POLKADOTS in p62-silenced D10 cells (7). We speculate that the small population of cells with residual Bcl10 clustering may reflect the activity of Nbr1, a protein functionally similar to p62 (18), which co-localizes with p62-speckles in T effector cells (7). Alternatively, the Carma1-dependent aggregation of Bcl10 (11) may inefficiently lead to the production of large cytosolic Bcl10 clusters in the absence of p62.

Finally, the percentage of $p62^{-/-}$ T_H2 cells that exhibited nuclear translocation of RelA was statistically significantly reduced compared to that of wild-type T_H2 cells in response to stimulation with anti-CD3/28 antibodies (Fig. 4, F and H), consistent with the observed reduction in IKK phosphorylation. Furthermore, those $p62^{-/-}$ T cells that exhibited nuclear translocation of RelA were the same cells that formed Bcl10-containing POLKADOTS (Fig. 4I). Moreover, the small population of responding $p62^{-/-}$ cells exhibited the same degree of RelA nuclear translocation as that of wild-type cells, as demonstrated by equivalent ratios of nuclear to cytosolic RelA (Fig. 4J). These data are consistent with our finding that the activation of NF-κB is digital; that is, that varying the intensity of TCR stimulation results in variations in the percentage of cells that respond, whereas the extent of activation of NF-κB on a per-cell basis is invariant in the responding population (10). These data suggest that p62 markedly enhances the efficiency of NF-κB signal transduction, increasing the percentage of effector T cells that successfully activate NF-κB in response to TCR stimulation. In the absence of p62, the activation of NF-κB is very inefficient, likely reflecting the near-absence of p62-dependent cytosolic clustering of Bcl10.

Discussion

Here, we showed that the stimulation of T cells led to the rapid redistribution of PKCθ and Carma1 to the immunological synapse. At early times after stimulation of the TCR, Bcl10 was recruited to both the immunological synapse and p62 speckles. Of note, the pIKK complex was enriched at these cytosolic p62-Bcl10-Malt1 aggregates (POLKADOTS), but not at the immunological synapse. TRAF6 was also enriched within the POLKADOTS structures. Cytosolic RelA and pIκBα also transiently colocalized with POLKADOTS clusters, which was followed by the persistent nuclear translocation of RelA. These data are consistent with the interpretation that IκBα–NF-κB complexes are recruited to the POLKADOTS signalosome, where activated IKK then phosphorylates IκBα. In additional experiments, we showed that inhibition of TAK1 and IKK activity had the predicted effects of blocking the TCR-dependent phosphorylation of IKK and the nuclear translocation of RelA, but had no effect on Bcl10 clustering to form the POLKADOTS signalosome. Thus, Bcl10 clustering is upstream of IKK activation. Finally, $p62^{-/-}$ T_H2 cells exhibited inefficient Bcl10 clustering, IKK phosphorylation, and RelA nuclear translocation; however they showed normal TCR-proximal signaling, suggesting that p62 plays a key role in the activation of the IKK complex in effector T cells. In contrast, naïve T cells from wild-type and $p62^{-/-}$ mice exhibited equivalent clustering of both Bcl10 and pIKKα/β beneath the crosslinked TCR, supporting a previous study that suggested that p62 does not play an essential role in TCR-dependent NF-κB signaling in naïve T cells (12). Together, these observations provide evidence that TCR signals direct the assembly of a p62-Bcl10-Malt1-TRAF6-IKK signalosome (the POLKADOTS signalosome), which stimulates the activation of NF-κB in effector T cells.

These findings establish a molecular mechanism that connects the CBM complex to the activation of NF-κB in effector T cells. Specifically, we showed that early, transient formation of the membrane-proximal CBM complex was followed by the assembly of the cytosolic POLKADOTS signalosome. A lingering question not directly resolved by our experiments is whether Carma1 is contained within the POLKADOTS signalosome. Although our antibody staining data suggest that Carma1 is enriched at the plasma membrane, and not at the POLKADOTS signalosome, other evidence suggests that POLKADOTS aggregates contain small amounts of Carma1. For example, structural studies show that activated Carma1 is required to initiate the Bcl10-polymerization process. Thus, although the resulting filaments are dominated by Bcl10, they also contain a few molecules of activated Carma1 at one end (11). Additionally, our previous FRET studies provided evidence that Carma1 is enriched within POLKADOTS structures (8), even though co-localization within POLKADOTS was not apparent by microscopy. We thus propose that Carma1 is activated at the plasma membrane by PKCθ-mediated phosphorylation. The resulting change in the conformation of Carma1 triggers the nucleation of Bcl10 filaments. The TCR-dependent, K63-linked polyubiquitination of Bcl10 also occurs in concordance with filament formation, leading to capture of filaments by cytosolic p62 speckles. The p62-dependent aggregation of filaments creates a large network of K63-linked polyubiquitin chains, which recruit IKK and the TAK1/TAB complex, ultimately resulting in the activation of TAK1 and IKK (19).

An unexpected observation in these studies relates to the distribution pattern of total IKKβ. In unstimulated D10 cells, IKKβ was primarily in cytoplasmic aggregates. After stimulation of cells with antigen, these aggregates persisted and were found to be proximal to, but rarely overlapping with, pIKKα/β at the POLKADOTS signalosome. The finding of aggregates of IKKβ in unstimulated cells is consistent with a recent study that reported that IKKγ-IKKβ exists in a very high molecular weight form in mouse embryonic fibroblasts and human embryonic kidney (HEK) 293T cells both before and after stimulation with tumor necrosis factor α (TNF-α) (16). The lack of correlation between the detection of total IKKβ and pIKKα/β could be explained by several alternative models, including direct or indirect interference of binding of anti-IKKβ by anti-pIKKα/β. However, because two distinct monoclonal antibodies against IKKβ yielded indistinguishable data, we believe it is unlikely that antibody interference accounts for our observations. Rather, we propose that the amount of pIKKα/β that translocates to POLKADOTS may be small in comparison to the amount of total IKKβ in the cytosolic aggregate pool, leading to undetectable anti-IKKβ staining in POLKADOTS.

Our data suggest that the TCR-dependent activation of NF-κB occurs at the POLKADOTS signalosome, and not at the cytosolic face of the TCR, where PKCθ and Carma1 are enriched. By providing a potential molecular mechanism for the cytosolic activation of IKK and NF-κB, these data may answer the question of how TCR signals are transduced from the membrane-associated CBM complex to the cytosolic IκBα-NF-κB complex. The assembly of distinct cytosolic signalosomes is emerging as a common, and perhaps essential, mechanism for transmitting activating signals to the IKK complex. Activating oligomers have been proposed as key intermediates upstream of IKK in the TNF-α receptor and the Toll-like receptor and IL-1 receptor signaling pathways (20), as well as in the retinoic acid-inducible gene-I (RIG-I)–mitochondrial antiviral signaling protein (MAVS) pathway (21), which induces NF-κB activation in response to viral RNA. In the case of TCR signaling to NF-κB, activated Carma1 induces the formation of oligomeric filaments of Bcl10 (11). Our data suggest that these filamentous polymers of Bcl10 are aggregated at the POLKADOTS signalosome, creating an IKK-activating signaling superstructure in effector T cells.

Our data show that efficient activation of IKK in effector T cells requires p62 and the POLKADOTS signalosome, because the absence of p62 led to poor Bcl10 clustering and minimal activation of IKK. How, then, does NF-κB activation occur in naïve T cells, which have a low abundance of p62 and activate NF-κB in a p62-independent manner (12)? Although there are not yet data to directly answer this question, it is clear that the CBM complex can activate NF-κB in naïve T cells without participation of the POLKADOTS signalosome. This difference in signaling architecture may reflect distinctions in the responses of naïve and effector cells to TCR-activating ligands. In this regard, a study demonstrated that naïve T cells require at least 20 hours of sustained signaling to enter the cell cycle, whereas sustained TCR signaling in effector T cells triggers apoptosis (22). Although there are probably several underlying mechanisms that account for these differences between naïve and effector cells (2), part of the explanation may be related to p62 playing a dual role in NF-κB activation (2, 7). Specifically, p62 is required both for the formation of the POLKADOTS signalosome, which activates IKK, and for limiting the activation of NF-κB through the selective autophagy of Bcl10 (7). Thus, the architecture of

the NF-κB signaling pathway in naïve T cells may be optimized to enable the continuous activation of NF-κB that is required to promote cell-cycle entry, whereas the switch to a reliance on p62 and the POLKADOTS signalosome in differentiated cells may both increase the efficiency of signal transmission and enable precise regulation of signal intensity and duration, preventing the deleterious consequences of sustained signaling to NF-κB, such as apoptosis, senescence, or both (23).

Because our data suggest that the POLKADOTS signalosome is a key regulator of NF-κB activation that may be unique to effector T cells, we believe that this structure is an attractive target for the development of immunomodulatory drugs. Although several NF-κB signaling pathways involve p62 (24), current data suggest that the p62-Bcl10 interaction is unique to effector T cells. The POLKADOTS signalosome is therefore likely to incorporate structurally unique features that may enable the rational design of inhibitors to block signal transmission to IKK and NF-κB. Through enabling highly specific inhibition of effector T cell activation, such drugs could have much use in the treatment of autoimmune diseases or other pathologies that are characterized by the undesired activation of effector T cells. It will therefore be important to define in molecular detail the composition and properties of this key signaling superstructure.

Materials and Methods

Mice and the differentiation of T_H2 cells

Tissues were harvested from 6- to 12-week-old C57BL/6 wild-type (WT) mice (National Cancer Institute) and $p62^{-/-}$ mice. The $p62^{-/-}$ strain (from ES cell clone EPD0162_1_G07) was obtained from the NIH–supported KOMP (knockout mouse project) Repository, generated by the CSD consortium for the NIH-funded KOMP, with established methodology (25). Harvesting of organs and the purification and in vitro differentiation of T_H2 cells were performed as described previously (7, 26). Briefly, $CD4^+$ T cells were isolated from lymph nodes from C57BL/6 WT or $p62^{-/-}$ mice by negative sorting with a CD4 isolation kit (Invitrogen). To differentiate naïve cells into T_H2 cells, naïve $CD4^+$ T cells were stimulated with plate-bound anti-CD3 and anti-CD28 antibodies in the presence of IL-2, IL-4, anti-IFN-γ antibody, and anti-IL-12 antibody for 4 days, which was followed by 2 days of culture in IL-2–containing medium to increase cell numbers. Animal experiments were approved by the USU Animal Care and Use Committee.

Antibodies

Primary antibodies used in this study were as follows: rabbit anti-Carma1 (Enzo, ALX-210-903), mouse anti-Bcl10 (Santa Cruz Biotechnology, sc-5273), rabbit anti-p62 (Sigma, P0067), mouse anti-tubulin (Santa Cruz Biotechnology, sc-5286), rabbit anti-PKCθ (Cell Signaling Technology), mouse anti-PKCθ (Enzo), anti-pERK1/2 (Cell Signaling Technology, 4370), mouse anti-GAPDH (Santa Cruz Biotechnology, sc-32233), mouse anti-tubulin (Santa Cruz Biotechnology, sc-5286), rabbit anti-pIKKα/β (Cell Signaling Technology, 2694), mouse anti-IKKβ (Imgenex, clone 10A9B6 (used in Fig. 1D) and clone 10AG2 (used in fig. S1B), mouse anti-TRAF6 (Santa Cruz Biotechnology, sc-8409), mouse anti-pIκBα (Cell Signaling Technology, 9246), and rabbit anti-RelA (Santa Cruz

Biotechnology, sc-372). Secondary antibodies included anti-rabbit and anti-mouse immunoglobulin G1 (IgG1) labeled with Alexa Fluor 488, Alexa Fluor 555, or Alexa Fluor 647 (Molecular Probes). Alexa Fluor 647–conjugated streptavidin (Molecular Probes) was used to crosslink anti-CD3 antibodies to induce TCR capping. DRAQ5 (Cell Signaling Technology) or DAPI [which is present in Prolong Gold mounting media (Invitrogen)], were used to mark the nucleus.

Cells, microscopy, and Western blotting

The D10 T_H2 cell clone and B cell lines (CH12 and CHb) were maintained in Eagle's Ham's Amino Acids (EHAA) medium with and without IL-2, respectively, as previously described (9). D10 cell lines expressing PKCθ, Bcl10, and Malt1 proteins fused to fluorescent proteins were previously described (8, 9). Formation of T cell–B cell conjugates was performed as previously described (7, 9). For experiments with SEB (a gift from C. Ventura and A. O'Brien), CHb cells were loaded with SEB (10 μg/ml) overnight, and then were centrifuged at 2000*g* for 30 s with an equal number of primary T_H2 cells. Stimulation of cells with anti-CD3 antibody alone or together with anti-CD28 antibody was performed as previously described (7). Capping of TCR on naïve T cells involved the use of biotinylated anti-CD3 antibody and Alexa Fluor 647–conjugated streptavidin, as previously described (3). For inhibitor experiments, T cells were incubated with 2 μM 5Z-7-oxozeaenol (Enzo) or DMSO (vehicle) 30 min before being stimulated, or with BAY 11-7082 (5 μg/ml, Calbiochem) 5 min after initiation of stimulation. For confocal microscopic analysis, cells were fixed and incubated with antibodies as previously described (8), and were visualized with a 40× 1.4 NA oil objective, a Zeiss 710 NLO microscope, and Zen software. Cell stimulation, harvesting, and Western blotting analysis were performed as previously described (7, 8).

Quantification of microscopy data

Raw data exported from Zeiss Zen software were analyzed with ImageJ software (US National Institutes of Health). For quantification of RelA nuclear occupancy, a region of interest (ROI) was drawn around the nucleus and cytoplasm of individual cells, using DRAQ5 or DAPI staining to define the nuclear periphery and the DIC image to define the plasma membrane (cytoplasm periphery). The mean pixel intensity of anti-RelA fluorescence within the nuclear and cytosolic ROIs was obtained for each cell and used to derive the nuclear/cytosolic RelA ratio. At least 20 cells were examined in each group. For quantifying POLKADOTS, cells with ≥2 Bcl10 clusters were scored as positive for POLKADOTS formation. Cells were scored as positive for nuclear RelA based on the presence of overlap of between RelA and DRAQ5 (or DAPI) fluorescence. At least 20 cells were counted in each group. GraphPad Prism 6.0 software was used to plot data and calculate errors and statistics.

Statistical analysis

Where indicated in the figure legends, *P* values for the differences in means were calculated with an unpaired, two-tailed Students *t* test.

Supplementary Material

Refer to Web version on PubMed Central for supplementary material.

Acknowledgments:

We thank A. Snow for antibodies and a critical reading of the manuscript.

Funding: This work was supported by grants from the US National Institutes of Health (Al057481 to B.C.S.), the Center for Neuroscience and Regenerative Medicine (to B.C.S), and pre-doctoral fellowships (to S.P.) from the American Heart Association (10PRE3150039) and the Henry M. Jackson Foundation.

References and Notes

1. Thome M, Charton JE, Pelzer C, Hailfinger S, Antigen receptor signaling to NF-kappaB via CARMA1, BCL10, and MALT1. Cold Spring Harb Perspect Biol 2, a003004 (2010). [PubMed: 20685844]
2. Paul S, Schaefer BC, A new look at T cell receptor signaling to nuclear factor-kappaB. Trends Immunol, (2013).
3. Gaide O, Favier B, Legler DF, Bonnet D, Brissoni B, Valitutti S, Bron C, Tschopp J, Thome M, CARMA1 is a critical lipid raft-associated regulator of TCR-induced NF-kappa B activation. Nat Immunol 3, 836–843 (2002). [PubMed: 12154360]
4. Bidere N, Snow AL, Sakai K, Zheng L, Lenardo MJ, Caspase-8 regulation by direct interaction with TRAF6 in T cell receptor-induced NF-kappaB activation. Curr Biol 16, 1666–1671 (2006). [PubMed: 16920630]
5. Sebald A, Mattioli I, Schmitz ML, T cell receptor-induced lipid raft recruitment of the I kappa B kinase complex is necessary and sufficient for NF-kappa B activation occurring in the cytosol. Eur J Immunol 35, 318–325 (2005). [PubMed: 15597322]
6. Carvalho G, Le Guelte A, Demian C, Vazquez A, Gavard J, Bidere N, Interplay between BCL10, MALT1 and IkappaBalpha during T-cell-receptor-mediated NFkappaB activation. J Cell Sci 123, 2375–2380 (2010). [PubMed: 20551178]
7. Paul S, Kashyap AK, Jia W, He YW, Schaefer BC, Selective autophagy of the adaptor protein Bcl10 modulates T cell receptor activation of NF-kappaB. Immunity 36, 947–958 (2012). [PubMed: 22658522]
8. Rossman JS, Stoicheva NG, Langel FD, Patterson GH, Lippincott-Schwartz J, Schaefer BC, POLKADOTS are foci of functional interactions in T-Cell receptor-mediated signaling to NF-kappaB. Mol Biol Cell 17, 2166–2176 (2006). [PubMed: 16495340]
9. Schaefer BC, Kappler JW, Kupfer A, Marrack P, Complex and dynamic redistribution of NF-kappaB signaling intermediates in response to T cell receptor stimulation. Proceedings of the National Academy of Sciences of the United States of America 101, 1004–1009 (2004). [PubMed: 14724296]
10. Kingeter LM, Paul S, Maynard SK, Cartwright NG, Schaefer BC, Cutting edge: TCR ligation triggers digital activation of NF-kappaB. J Immunol 185, 4520–4524 (2010). [PubMed: 20855880]
11. Qiao Q, Yang C, Zheng C, Fontan L, David L, Yu X, Bracken C, Rosen M, Melnick A, Egelman EH, Wu H, Structural Architecture of the CARMA1/Bcl10/MALT1 Signalosome: Nucleation-Induced Filamentous Assembly. Mol Cell 51, 766–779 (2013). [PubMed: 24074955]
12. Martin P, Diaz-Meco MT, Moscat J, The signaling adapter p62 is an important mediator of T helper 2 cell function and allergic airway inflammation. EMBO J 25, 3524–3533 (2006). [PubMed: 16874300]
13. Schaefer BC, Kappler JW, Kupfer A, Marrack P, Complex and dynamic redistribution of NF-kappaB signaling intermediates in response to T cell receptor stimulation. Proc Natl Acad Sci U S A 101, 1004–1009 (2004). [PubMed: 14724296]

14. Sun L, Deng L, Ea CK, Xia ZP, Chen ZJ, The TRAF6 ubiquitin ligase and TAK1 kinase mediate IKK activation by BCL10 and MALT1 in T lymphocytes. Mol Cell 14, 289–301 (2004). [PubMed: 15125833]
15. Vallabhapurapu S, Karin M, Regulation and function of NF-kappaB transcription factors in the immune system. Annu Rev Immunol 27, 693–733 (2009). [PubMed: 19302050]
16. Polley S, Huang DB, Hauenstein AV, Fusco AJ, Zhong X, Vu D, Schrofelbauer B, Kim Y, Hoffmann A, Verma IM, Ghosh G, Huxford T, A structural basis for IkappaB kinase 2 activation via oligomerization-dependent trans auto-phosphorylation. PLoS Biol 11, e1001581 (2013). [PubMed: 23776406]
17. Shambharkar PB, Blonska M, Pappu BP, Li H, You Y, Sakurai H, Darnay BG, Hara H, Penninger J, Lin X, Phosphorylation and ubiquitination of the IkappaB kinase complex by two distinct signaling pathways. EMBO J 26, 1794–1805 (2007). [PubMed: 17363905]
18. Yang JQ, Liu H, Diaz-Meco MT, Moscat J, NBR1 is a new PB1 signalling adapter in Th2 differentiation and allergic airway inflammation in vivo. The EMBO Journal 29, 3421–3433 (2010). [PubMed: 20808283]
19. Chen ZJ, Ubiquitination in signaling to and activation of IKK. Immunol Rev 246, 95–106 (2012). [PubMed: 22435549]
20. Napetschnig J, Wu H, Molecular basis of NF-kappaB signaling. Annu Rev Biophys 42, 443–468 (2013). [PubMed: 23495970]
21. Hou F, Sun L, Zheng H, Skaug B, Jiang QX, Chen ZJ, MAVS forms functional prion-like aggregates to activate and propagate antiviral innate immune response. Cell 146, 448–461 (2011). [PubMed: 21782231]
22. Iezzi G, Karjalainen K, Lanzavecchia A, The duration of antigenic stimulation determines the fate of naive and effector T cells. Immunity 8, 89–95 (1998). [PubMed: 9462514]
23. Zhi H, Yang L, Kuo YL, Ho YK, Shih HM, Giam CZ, NF-kappaB hyper-activation by HTLV-1 tax induces cellular senescence, but can be alleviated by the viral anti-sense protein HBZ. PLoS Pathog 7, e1002025 (2011). [PubMed: 21552325]
24. Moscat J, Diaz-Meco MT, p62 at the crossroads of autophagy, apoptosis, and cancer. Cell 137, 1001–1004 (2009). [PubMed: 19524504]
25. Testa G, Schaft J, van der Hoeven F, Glaser S, Anastassiadis K, Zhang Y, Hermann T, Stremmel W, Stewart AF, A reliable lacZ expression reporter cassette for multipurpose, knockout-first alleles. Genesis 38, 151–158 (2004). [PubMed: 15048813]
26. Kingeter LM, Schaefer BC, Loss of protein kinase C theta, Bcl10, or Malt1 selectively impairs proliferation and NF-kappa B activation in the CD4+ T cell subset. J Immunol 181, 6244–6254 (2008). [PubMed: 18941215]

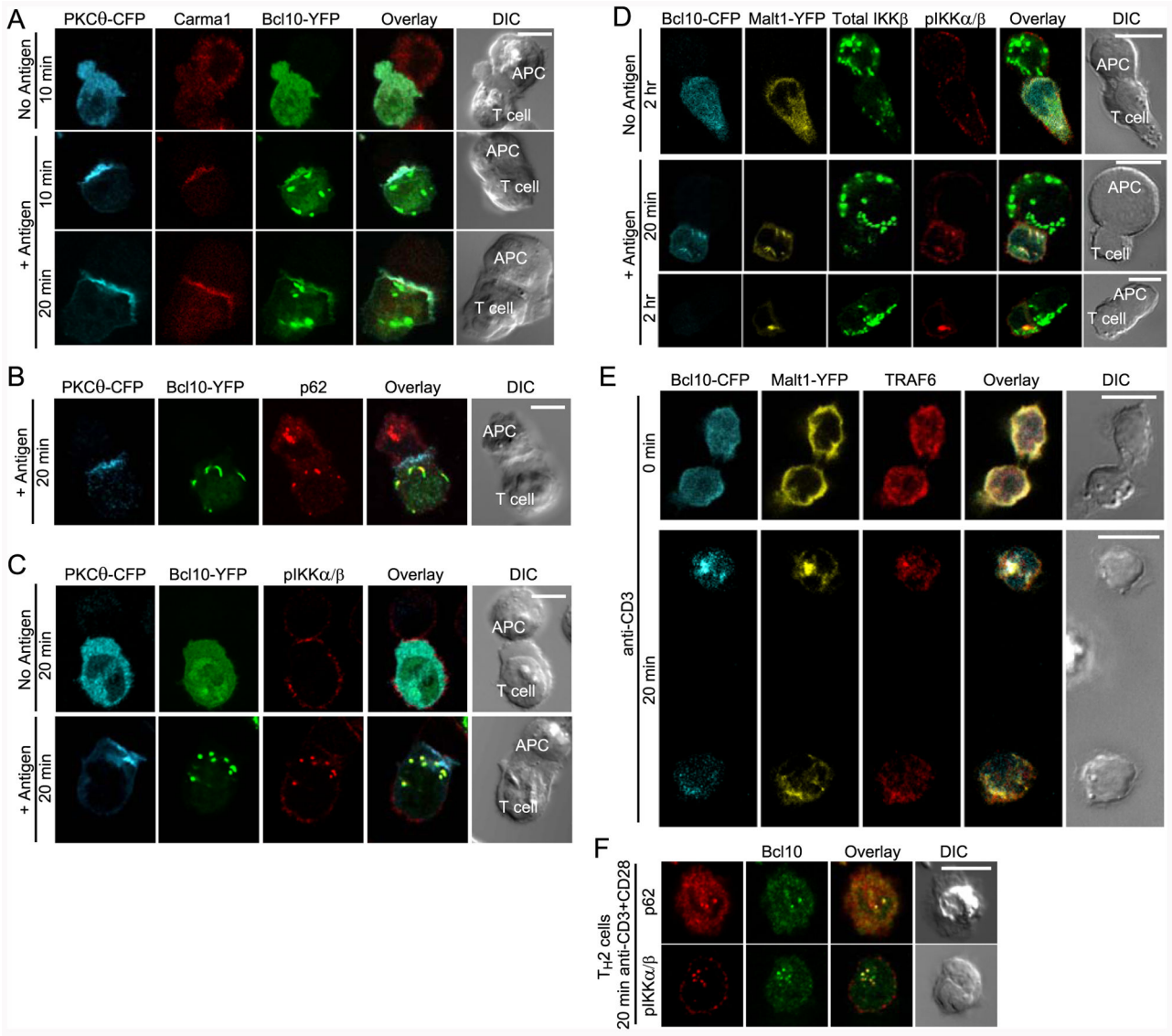

Fig. 1. Colocalization of pIKKα/β and TRAF6 with cytosolic Bcl10-p62 clusters after TCR stimulation.

(**A** to **C**) D10 cells transduced with retroviruses encoding PKCθ-CFP and Bcl10-YFP were stimulated for the indicated times by CH12 cells that were either not loaded (No Antigen) or were loaded with conalbumin (+ Antigen). Cells were then analyzed by confocal microscopy. Fluorescent proteins and antibody stains are indicated above each image. (**D** and **E**) D10 cells transduced with retroviruses encoding Bcl10-CFP and Malt1-YFP were left untreated or were stimulated for the indicated times with (D) CH12 cells that were either not loaded (No Antigen) or were loaded with conalbumin (+ Antigen) or (E) anti-CD3 antibody. Cells were then stained with antibodies against the indicated proteins before being analyzed by confocal microscopy. (**F**) Primary mouse naïve $CD4^+$ T cells were differentiated in vitro into T_H2 cells and then were incubated on coverslips coated with anti-CD3 and anti-CD28 antibodies. Cells were then stained with antibodies against the indicated proteins and

analyzed by confocal microscopy. All images are representative of three or four independent experiments. Scale bar: 10 μm.

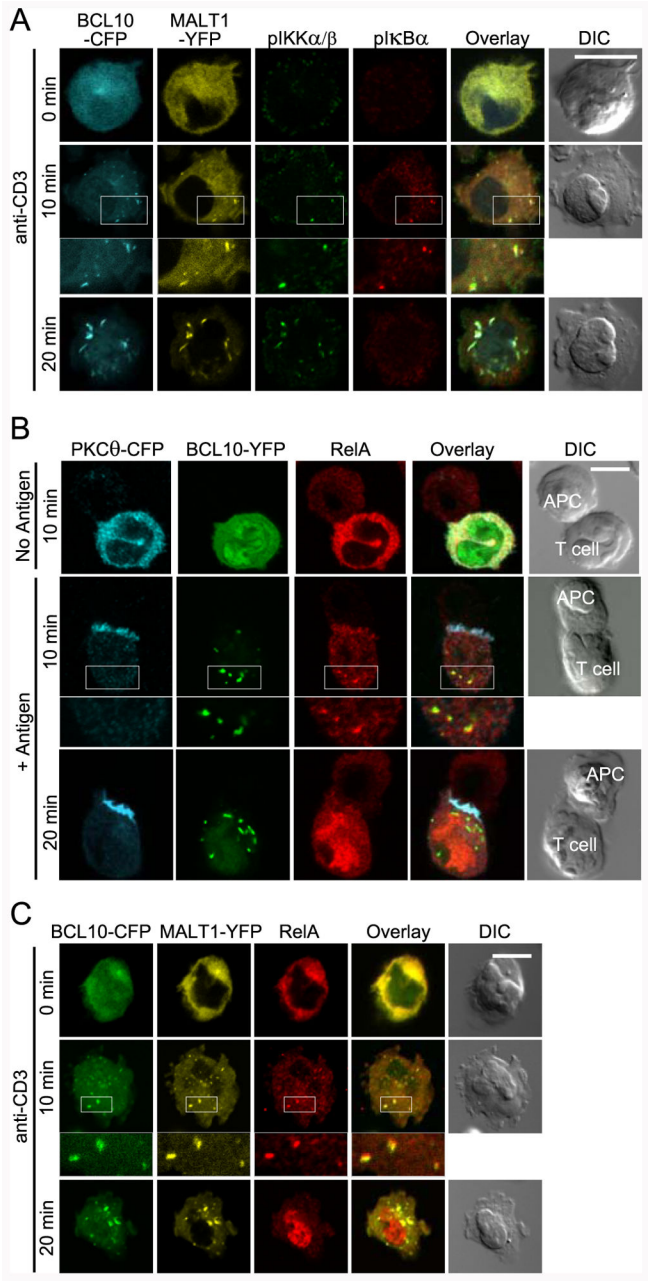

Fig. 2. pIκBα and RelA exhibit transient colocalization with cytosolic Bcl10-containing signalosomes before translocating to the nucleus.

(**A**) D10 cells transduced with retroviruses encoding Bcl10-CFP and Malt1-YFP were left untreated or were stimulated with anti-CD3 antibodies. Cells were then stained with antibodies against the indicated proteins, and analyzed by confocal microscopy. (**B**) D10 cells transduced with retroviruses encoding PKCθ-CFP and Bcl10-YFP were stimulated for the indicated times with CH12 cells that were either unloaded (No Antigen) or were loaded with conalbumin (+ Antigen). Cells were then stained with anti-RelA and analyzed by confocal microscopy. (**C**) D10 cells transduced with retroviruses encoding Bcl10-CFP and Malt1-YFP were left untreated or were stimulated with anti-CD3 antibodies. Cells were then

stained with anti-RelA and analyzed by confocal microscopy. Inset images below the 10-min time points are magnified views of the areas marked by white rectangles. All of the images are representative of at least four independent experiments. Scale bar: 10 μm.

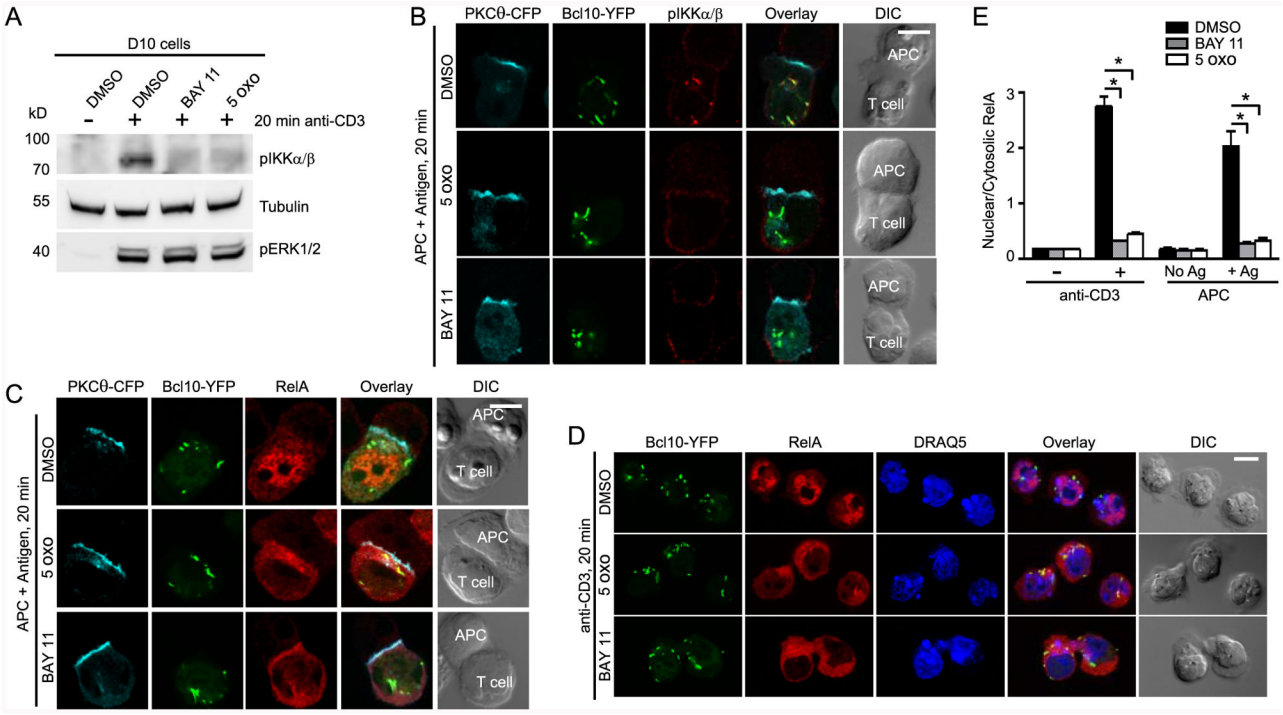

Fig. 3. Inhibition of TAK1 or IKK blocks IKK phosphorylation and RelA activation, but not Bcl10 clustering.

(**A**) D10 cells were treated with DMSO (control), BAY 11-7082 (BAY 11), or 5Z-7-oxozeaenol (5 oxo) before being stimulated with anti-CD3 antibody for 20 min. Cells were then lysed and analyzed by Western blotting with antibodies against the indicated proteins. Migration of molecular mass markers (kD) is indicated to left. Data are representative of three independent experiments. (**B** to **D**) D10 cells transduced with retroviruses encoding PKCθ-CFP and Bcl10-YFP were treated with DMSO (control), BAY 11, or 5 oxo, and were stimulated with (B and C) antigen-loaded CH12 cells (APCs) or (D) anti-CD3 antibody. Cells were then stained with antibodies against the indicated proteins and were analyzed by confocal microscopy. See fig. S2 for control images. DRAQ5 was used to stain nuclear DNA in (D). (**E**) The ratios of the abundances of nuclear and cytosolic RelA protein were quantified in cells from the experiments shown in (C) and (D). At least 20 cells were quantified in each group. Data are means ± SEM. *$P < 0.05$. Images in (B to D) are representative of three independent experiments. Scale bar: 10 μm.

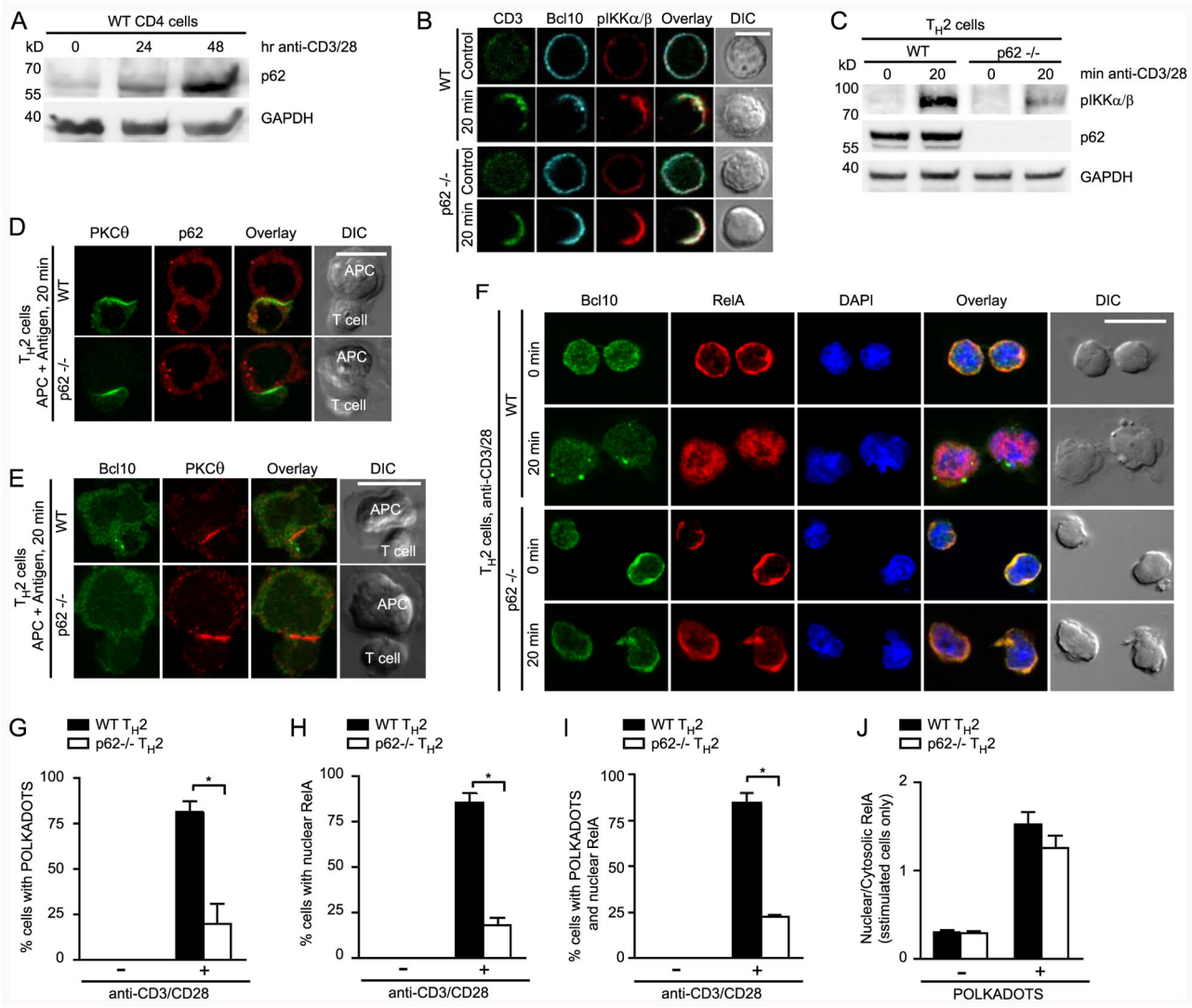

Fig. 4. p62 is required for efficient cytosolic Bcl10 clustering, IKK phosphorylation, and RelA nuclear translocation in primary effector T cells.

(**A**) Naïve $CD4^+$ T cells isolated from WT C57BL/6 mice were stimulated with plate-bound anti-CD3 and anti-CD28 antibodies, lysed, and then analyzed by Western blotting with antibodies against the indicated proteins. (**B**) Lymph node cells isolated from WT or $p62^{-/-}$ mice were incubated on ice with biotinylated anti-CD3 antibody, which was followed by streptavidin-induced crosslinking on ice (control) or at 37°C (for 20 min). The cells were then fixed and stained with antibodies against the indicated proteins. (**C**) Primary T_H2 cells derived from WT or $p62^{-/-}$ mice were stimulated with plate-bound anti-CD3 and anti-CD28 antibodies, lysed, and analyzed by Western blotting with antibodies against the indicated proteins. (A and C) Migration of molecular mass markers (kD) is indicated to left. Blots are representative of two independent experiments. (**D** and **E**) T_H2 cells derived from WT or $p62^{-/-}$ mice were stimulated with SEB-loaded CHb cells (APCs), stained with the antibodies against the indicated proteins, and then analyzed by confocal microscopy. Note that the p62 speckles in (D) are present only in the CHb cells. (**F**) T_H2 cells derived from

WT or p62$^{-/-}$ mice were stimulated on coverslips coated with anti-CD3 and anti-CD28 antibodies for 20 min, and stained with antibodies against the indicated proteins and DAPI (to visualize nuclei). Cells were then analyzed by confocal microscopy. (**G** to **I**) Data from the experiment in (F) were quantified. Graphs show the percentages of cells that exhibited (G) cytosolic Bcl10 clusters (POLKADOTS) alone, (H) nuclear RelA alone, or (I) both. (**J**) Graph showing the ratios of the staining intensities of nuclear and cytosolic RelA in anti-CD3– and anti-CD28–stimulated WT and p62$^{-/-}$ T_H2 cells that did or did not exhibit cytosolic POLKADOTS. At least 20 cells were quantified in each group. Data in bar graphs are means ± SEM. *P <0.05. Data in each panel are representative of two independent experiments. Scale bar: 5 μm (for B) or 10 μm (for D to F).